Electronic Supplementary Information

Large-scale synthesis of ceria-based nano-oxides with high CO oxidation activity

Pankaj Bharali,[a,b] Pranjal Saikia[a,c] and Benjaram M. Reddy[a,*]

[a] *Inorganic and Physical Chemistry Division, Indian Institute of Chemical Technology, Hyderabad 500 607, India*

[b] *Department of Chemical Sciences, Tezpur University, Napaam, Tezpur 784 028, India*

[c] *Department of Chemical Science, Institute of Science and Technology, Gauhati University, Guwahati 781 001, India*

* Correspondence to Benjaram M. Reddy (bmreddy@iict.res.in; mreddyb@yahoo.com)

Experimental Procedures

***Synthesis*:** The precursors employed [$(NH_4)_2Ce(NO_3)_6$ (Loba Chemie, GR grade), $Zr(NO_3)_4.5H_2O$ (Fluka, AR grade), $HfCl_4$ (Aldrich, AR grade), $Tb(NO_3)_3$ (Aldrich, AR grade), powder form of γ-Al_2O_3 (< 50 μm, Harshaw Chem.)] in the synthesis of the materials were used as obtained without further purification. The materials are synthesized in 5 g batch and can be scaled up for large quantities.[SR1] In a typical procedure, powdered γ-Al_2O_3 (specific surface area of 127 m^2g^{-1}) is first dispersed in about 2000 mL deionized water and stirred for 2 h. Separately, calculated quantities of the metal precursors are

dissolved in 200 mL deionized water and stirred for 2 h. Subsequently, the appropriate solutions are added drop-wise to the dispersed alumina suspension under continuous stirring. Finally, the whole mixture solution is diluted to approximately 4000 mL with deionized water. The stirring is continued for another 1 h. Aqueous NH_3 solution (28% NH_3 diluted with deionized water) is added drop-wise to the mixture solution until pH ~8.5, under vigorous stirring. The obtained precipitate is filtered off, washed with ca. 3000 mL deionized water and oven dried at 393 K for 12 h, and subsequently calcined at 773 K for 5 h in air atmosphere to obtain the final materials.

***Powder X-ray Diffraction*:** Powder X-ray diffraction patterns are recorded using a Rigaku Multiflex instrument equipped with nickel-filtered Cu Kα (0.15418 nm) radiation source and a scintillation counter detector. The intensity data are collected over a 2θ range of 2 –80° with a 0.02° step size and using a counting time of 1 s per point. The XRD phases present in the samples are identified with the help of Powder Diffraction File-International Center for Diffraction Data (PDF-ICDD). The average crystallite size of the oxide phases is estimated with the help of Scherrer equation and the lattice parameter is calculated by a standard cubic indexation method using the intensity of the most prominent peak (111).

***Transmission Electron Microscopy*:** The TEM–HREM studies are made on a JEM-2010 (JEOL) instrument equipped with a slow-scan CCD camera and at an accelerating voltage of 200 kV. Samples are sonically dispersed in ethanol and deposited on a carbon-coated copper grid before examination.

***BET Surface Area*:** The BET surface areas are determined by N_2 physisorption at liquid N_2 temperature, on a Micromeritics Gemini 2360 instrument. Prior to analysis, the samples are oven-dried at 393 K for 12 h and flushed with Argon gas for 2 h.

***Raman Spectra*:** The Raman spectra are recorded with a LabRam HR800UV Raman spectrometer (Horiba Jobin-Yvon) equipped with a confocal microscope and liquid-nitrogen cooled charge-coupled device (CCD) detector. The emission line at 325 nm from He-Cd laser (Melles Griot Laser) is focused on the sample under the microscope, with the diameter of the analyzed spot being ~1 μm. The time of acquisition is adjusted according to the intensity of Raman scattering. The wavenumber values reported from the spectra are accurate to within 1 cm^{-1}. In order to ascertain the homogeneity of the sample, spectra are recorded at various points and compared. All samples are found to be highly homogeneous.

***UV-visible Diffuse Reflectance Spectroscopy*:** The UV–vis DRS measurements are performed over the wavelength range 200–700 nm using a GBS-Cintra 10e UV–vis NIR spectrophotometer with integration sphere diffuse reflectance attachment. Samples are diluted in a KBr matrix by pelletization.

***X-ray Photoelectron Spectroscopy*:** The XPS measurements are made on a Shimadzu (ESCA 3400) spectrometer by using Mg Kα (1253.6 eV) radiation as the excitation source. Charging of samples is corrected by setting the binding energy maximum of the

adventitious carbon (C 1s) at 284.6 eV. The analysis was performed at room temperature and pressures are typically in the order of less than 10^{-8} Pa. The samples are out gassed in a vacuum oven overnight before XPS measurements.[SR2,SR3]

***Ion Scattering Spectroscopy*:** IS spectra are measured with a Leybold surface analysis system equipped with X-ray and ion sources and an EA 10/100 electron (ion) analyzer with multichannel detection (Specs). The samples are pretreated in flowing synthetic air (20% O_2/N_2) at 573 K for 30 min before they are introduced into the spectrometer vacuum without further contact with the ambient humid atmosphere (in-situ treatment). The measurements are carried out with 3000 eV Ar+ ions and recorded with the analyzer in pass-energy mode. The surface charge is removed with a flood gun. The source and the flood gun are allowed to stabilize with the sample withdrawn from the measurement position. Signal intensities are estimated assuming the background to be linear.

***Temperature Programmed Reduction*:** The TPR measurements are performed in a system equipped with a thermal conductivity detector. Before starting TPR runs, the sample is activated under flowing O_2 (9.35%)/Ar at 573 K for 30 min maintaining the heating rate at 10 K min^{-1}. The sample is then cooled to starting temperature. TPR is performed by heating the sample at 5 K min^{-1} up to 1073 K in a H_2 (4.2%)/Ar flow (84.1 mL min^{-1}).

***CO Oxidation Measurements*:** The CO oxidation activity of the synthesized materials is evaluated at normal atmospheric pressure and temperatures in the range of 300–773 K in a

fixed bed micro-reactor at a heating ramp of 5 K min^{-1}.[SR2-SR4] About 100 mg of the sample (250–355 μm sieve fraction) diluted with quartz particles of the same sieve fraction is placed in a quartz reactor for evaluation. Temperature is measured directly at the catalyst bed, using a thermocouple placed in the hollow part of the reactor. The following gases and gas mixtures are used (supplied by Air Liquide): argon (>99.999% purity), 9.98% CO in argon (CO purity, >99.997%; argon purity, >99.99%), and 10.2% O_2 in argon (oxygen purity, >99.995%). The total flow rates maintained by three mass flow controllers are in the range of 50–60 NmL min^{-1} (milliliters normalized to 273.15 K and 1 atm.). The CO and CO_2 gas concentrations were measured using an Uras 14 infrared analyzer module, and the O_2 concentration is measured using a Magnos 16 analyzer (Hartmann & Braun). Prior to oxidation of CO, the catalysts are heated to 773 K in 10.2% O_2/Ar gas mixture, using a heating ramp of 10 K min^{-1}, and kept at the final temperature for 1 h. The oxidized sample is then purged in argon and cooled to the desired starting temperature. The CO/O_2 reactant feed ratio is 1, and partial pressures of CO and O_2 are in the range of 10 mbar. The conversion of CO iss calculated using the following equation.

$$\text{CO conversion (\%)} = \frac{[CO]_{in} - [CO]_{out}}{[CO]_{in}} \times 100$$

***Oxygen Storage Capacity Measurements*:** A thermogravimetric method, essentially similar to that described previously elsewhere,[SR2-SR7] is used to determine the OSC by the oxygen release characteristics of the sample in the temperature region 573–1073 K. The

change in the weight of the sample is monitored by thermogravimetry (TG) under cyclic heat treatments in flowing nitrogen or dry air. A commercial Netzsch TG–DTA analyzer (Luxx, STA, 409 PC, Germany) is employed for this purpose. The heat cycle consisted of heating the sample to 1073 K, cooling to 423 K, and again heating to 1073 K. All heating and cooling rates are maintained at 5 K min^{-1}. The weight loss of the sample during the second heating cycle is used to measure the oxygen release properties.

Supporting References:

(SR1) B. M. Reddy, A. Khan, P. M. Sreekanth and P. Lakshmanan, *U.S. Patent 0025301*. Feb. 2006.

(SR2) B. M. Reddy, P. Saikia, P. Bharali, S.-E. Park, M. Muhler and W. Grünert, *J. Phys. Chem. C* 2009, **113**, 2452 – 2462.

(SR3) B. M. Reddy, P. Bharali, P. Saikia, S.-E. Park, M. W. E. van den Berg, M. Muhler and W. Grünert, *J. Phys. Chem. C* 2008, **112**, 11729 – 11737.

(SR4) B. M. Reddy, P. Lakshmanan, P. Bharali, P. Saikia, G. Thrimurthulu, M. Muhler and W. Grünert, *J. Phys. Chem. C* 2007**, 111**, 10478 – 10483.

(SR5) B. M. Reddy, P. Bharali, P. Saikia, A. Khan, S. Loridant, M. Muhler and W. Grünert, *J. Phys. Chem. C* 2007, **111**, 1878 – 1881.

(SR6) M. Ozawa, K. Matuda and S. Suzuki, *J. Alloys Compd.* 2000, **303-304**, 56 – 59.

(SR7) B. M. Reddy, G. Thrimurthulu, L. Katta, Y. Yamada and S.-E. Park, *J. Phys. Chem. C* 2009, **113**, 15882 – 15890.

***Fig. S1*:** TEM images of (A) $Ce_{0.8}Hf_{0.2}O_2/Al_2O_3$ and (B) $Ce_{0.75}Zr_{0.25}O_2/Al_2O_3$.

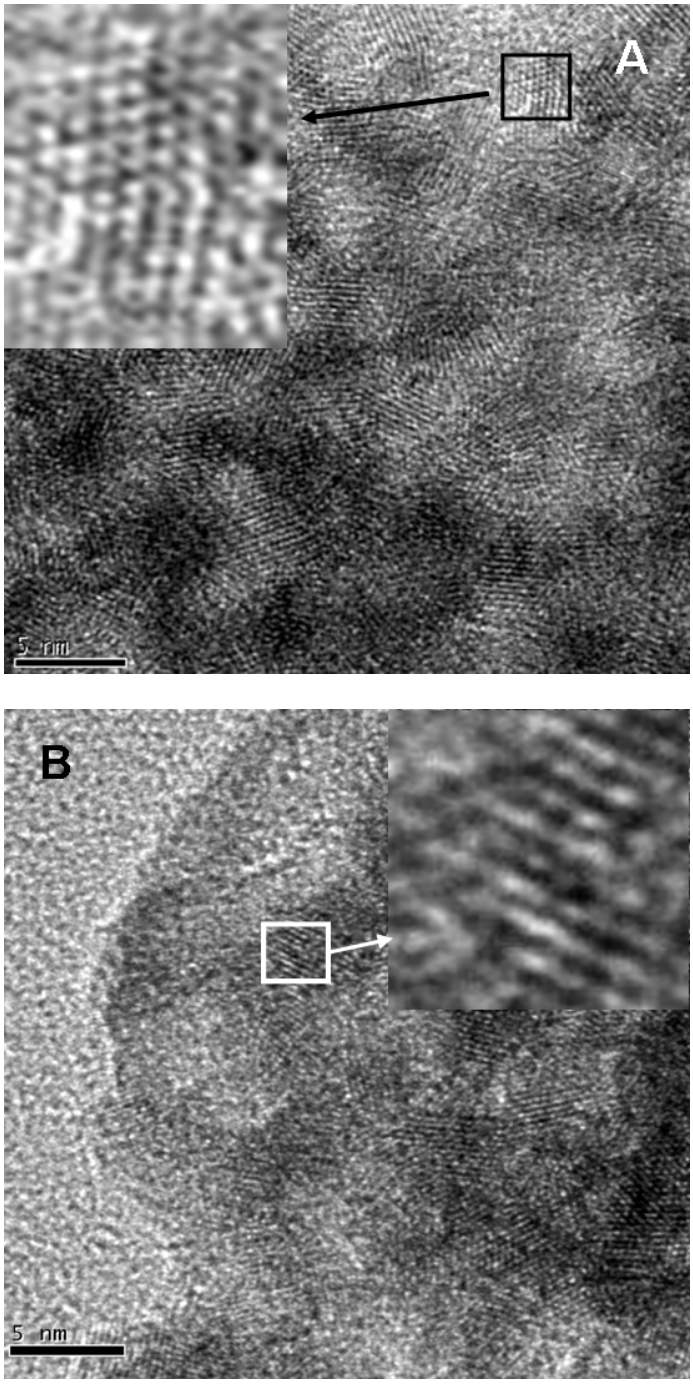

***Fig. S2*:** Ultraviolet-Raman spectra of Al_2O_3 supported $Ce_{0.8}Tb_{0.2}O_2$ (CTA), $Ce_{0.8}Hf_{0.2}O_2$ (CHA), and $Ce_{0.75}Zr_{0.25}O_2$ (CZA). The inset shows the UV-Raman spectra of pure CeO_2.

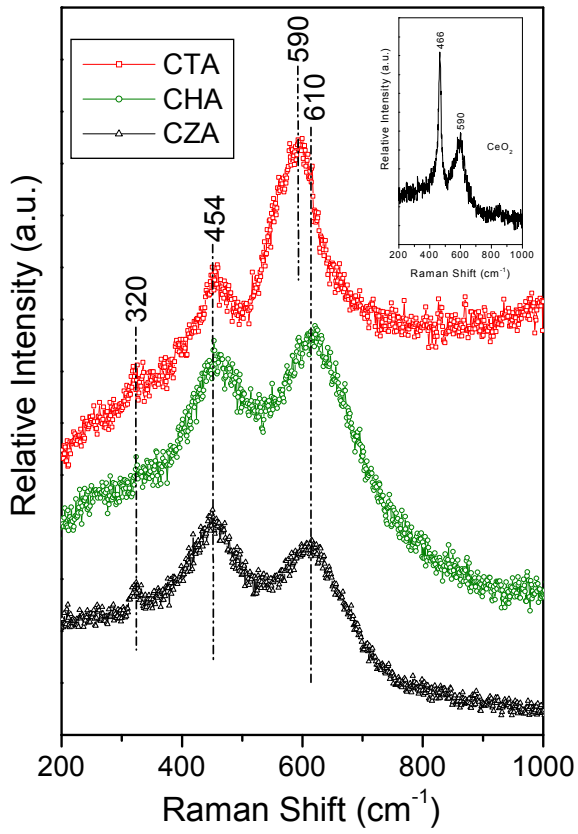

Additional information related to Fig. S2: Raman spectroscopy is one of the most useful techniques for characterization of materials and to gather information on both M–O bond arrangement and lattice defects. It is well reported in the literature that the intensity of Raman bands may vary depending on the laser source used. Based on the fact that the laser with shorter wavelength is closer to the electronic adsorption of samples, it was reported that the Raman information detected by excitation laser with shorter wavelength is more sensitive to the surface region of the samples. We have used a UV excitation laser (He-Cd laser) with wavelength 325 nm in the present investigation. Moreover, in the present investigation the synthesized samples showed strong absorption in the UV region as observed from UV-vis DRS (Fig. S3). Therefore, we suggest that the bands corresponding

to the oxygen vacancy formation in the oxides are related to the surface region. All samples show two main peaks in the region of ~450 and ~600 cm^{-1}, the peak at 450 cm^{-1} was related to the F_{2g} vibrational mode, characteristic of the cubic fluorite-structure. It can be viewed as symmetric breathing mode of oxygen atoms of CeO_8 unit of ceria lattice. The peak at 600 cm^{-1} is attributed to lattice defects, resulting from the formation of oxygen vacancies, which allows this mode of vibration by relaxation of selection rules. This peak is less prominent in the ceria sample (inset in figure), while it became major in the CTA with a slight shift than the CHA and CZA. It could be due to more oxygen vacancies introduced to provide charge balance for the presence of Tb cations and the increased Ce^{3+} ions. It is observed that the characteristic F_{2g} vibrational mode is shifted to lower frequencies and broadened when the Tb, Hf, and Zr cations introduced into the CeO_2 lattice. Besides, there is another weak band at around 320 cm^{-1} which is assigned to the displacement of oxygen atoms from their ideal fluorite lattice positions.

Additional information related to Fig. S3: It is known that pure CeO_2 exhibits three absorption maxima centered at ~255, 285, and 340 nm in its UV-vis DR spectra. The latter two absorption maxima are ascribed to $Ce^{4+} \leftarrow O^{2-}$ charge transfer and inter-band transitions, respectively. The former maxima corresponds to $Ce^{3+} \leftarrow O^{2-}$ charge transfer transitions. Specular reflectance effects produced by the strong absorption of ceria in the UV range may lead to such nature of the patterns. Though it might affect the shape of the inter-band transition, the absorption edge position has not been modified remarkably. In the present case, the absorption edges are blue shifted with respect to ceria. This blue shift may be the result of decreasing particle size of ceria (quantum size effect) when Tb^{4+}, Hf^{4+}, and Zr^{4+} ions are incorporated into the ceria lattice as evidenced by XRD analysis. Also, it may be due to an increasing contribution of $Ce^{4+} \leftarrow O^{2-}$ charge transfer which is more prominent in case of smaller crystallites (localized effect). It is interesting to note that the band at ~250 nm, which has been characterized as $Ce^{3+} \leftarrow O^{2-}$ charge transfer transition, is also well resolved in case of CTA and CHA samples. This implies the occurrence of oxygen vacancy defects in the samples corroborating with the Raman spectroscopy studies.

Besides, there is a hump in the DRS profile of CTA showing a transition of Tb cation in the visible region.

***Fig. S3*:** Ultraviolet-visible diffuse reflectance spectra (UV-vis DRS) of Al_2O_3 supported $Ce_{0.8}Tb_{0.2}O_2$ (CTA), $Ce_{0.8}Hf_{0.2}O_2$ (CHA), and $Ce_{0.75}Zr_{0.25}O_2$ (CZA) showing various ligand to metal charge transfer transitions (LMCT) and other transitions.

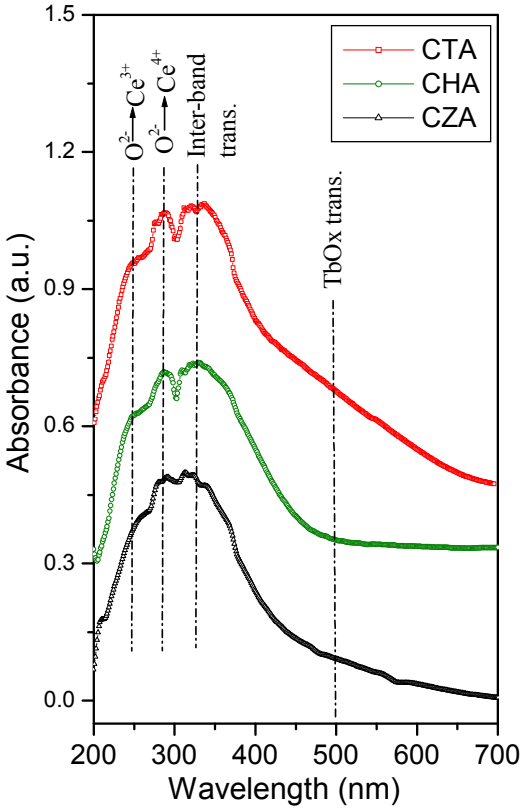

***Fig. S4*:** X-ray photoelectron spectra (XPS) of Ce 3d core photoelectrons of Al_2O_3 supported $Ce_{0.8}Tb_{0.2}O_2$ (CTA), $Ce_{0.8}Hf_{0.2}O_2$ (CHA), and $Ce_{0.75}Zr_{0.25}O_2$ (CZA).

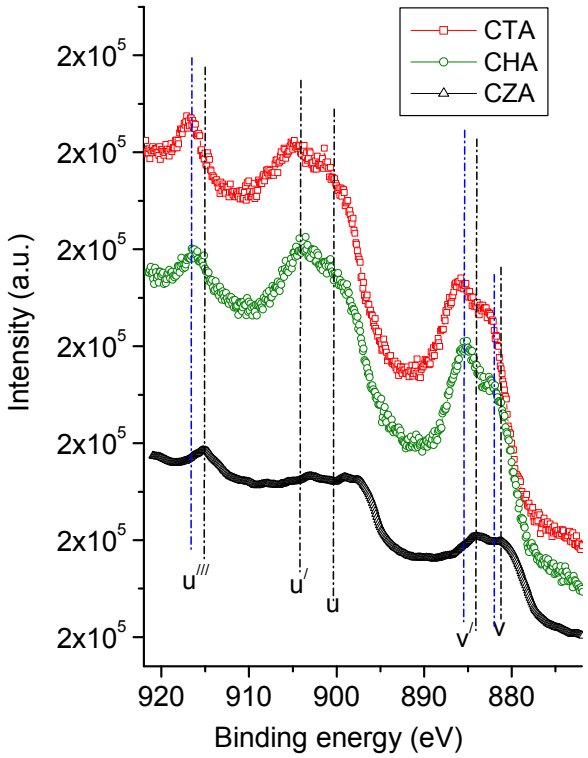

Additional information related to Fig. S4: Due to the hybridization of the O 2p valence band with Ce 4f level, Ce 3d core level XPS pattern of ceria is very complicated resulting in several final states and a number of overlapping peaks. As can be seen from the Fig. S4, the Ce 3d spectra consists of two sets of spin-orbit multiplets featuring $3d_{3/2}$ and $3d_{5/2}$ (represented as u and v, respectively) contributions. The peaks at ~882 eV (v) and 901 eV (u) are the main lines corresponding to Ce^{4+} state whereas features at ca. 888.5 eV (v''), 898 eV (v'''), 907 eV (u'') and 916.8 eV (u''') are satellites related to this state. The main signals of Ce^{3+} (v_0 and u_0) are generally noticed at around 881 and 898 eV, respectively. Here, it can be seen that the latter peak is overlapping with v'''. The satellites to these features (v' and u') occur at 885.9 and 904.2 eV, respectively. It can be observed that the peak at ~881 eV (characteristic of Ce^{3+}) is very meager in all the spectra showing the

presence of Ce predominantly in the 4+ oxidation state. This is again supported by the considerable intensity of the u''' peak. Interestingly, significant peak intensity is observed at ~885 eV indicating the presence of Ce^{3+} in the sample. Thus, on the surface of the samples, Ce is present in both Ce^{4+} and Ce^{3+} oxidation states. It was clearly observed the differences in the Ce 3d patterns of CTA and CHA with CZA with some shifts in the peak positions as marked by pink color. The shifts in the peak positions demarcate the differences in the surface composition of the Ce content in various oxidation states and eventually support the activity results.

***Fig. S5*:** X-ray photoelectron spectra (XPS) of (a) Al 2p and (b) O 1s photoelectrons of Al_2O_3 supported $Ce_{0.8}Tb_{0.2}O_2$ (CTA), $Ce_{0.8}Hf_{0.2}O_2$ (CHA), and $Ce_{0.75}Zr_{0.25}O_2$ (CZA).

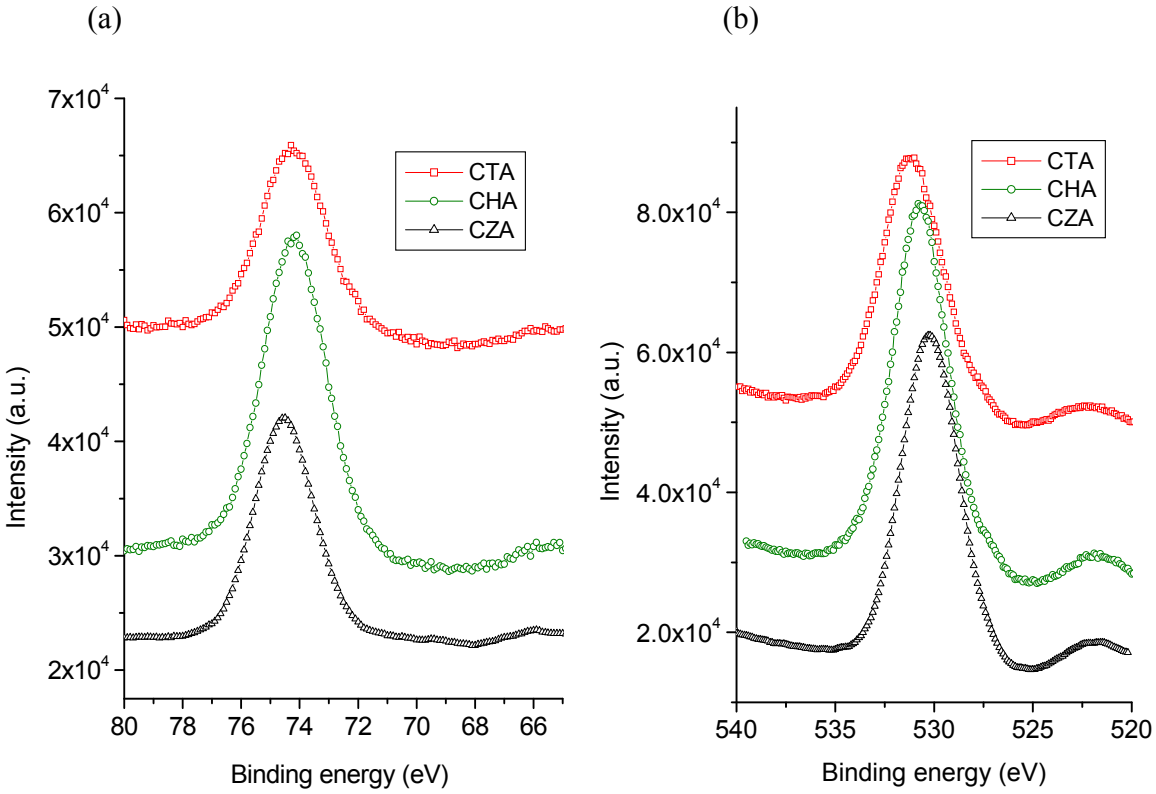

<u>Additional information related to Fig. S5</u>: The binding energy of Al^{3+} in alumina is observed at 74.2–74.5 eV as can be seen in the Fig. S5 (a) which is in the range of binding

energies (73.7–74.8 eV) reported for Al 2p core level of alumina. The XPS profiles of O 1s core electron levels of all the samples are shown in Fig. S5 (b). As can be observed, all the patterns consist of broad peaks centered at 530–531 eV assigned to lattice oxygen associated with the oxides. The asymmetric nature of the peaks can be attributed to the different environments for oxides that constitute the materials. The very flat nature of the peaks may mask any probable shoulder towards the high binding energy side which is more likely to be present due to absorbed oxygen or surface hydroxyl species and/or absorbed water present as contaminant at the surface.

***Fig. S6*:** Plot of Tb/Ce intensity ratio obtained for Al_2O_3 supported $Ce_{0.8}Tb_{0.2}O_2$ (CTA) oxide after different scans.